

# Quantification of Wheat Straw Lignin Structure by Comprehensive NMR Analysis

Jijiao Zeng,<sup>†</sup> Gregory L. Helms,<sup>‡</sup> Xin Gao,<sup>†</sup> and Shulin Chen<sup>\*†</sup>

<sup>†</sup>Department of Biological Systems Engineering, The Bioprocessing and Bioproduct Engineering Laboratory (BBEL), L. J. Smith 213, Washington State University, Pullman, Washington 99163 United States

<sup>‡</sup>Department of Chemistry, The Center for NMR Spectroscopy, Washington State University, Pullman, Washington 99163, United States

**ABSTRACT:** A further understanding of the structure of lignin from herbaceous crops is needed for advancing technologies of lignocellulosic biomass processing and utilization. A method was established in this study for analyzing structural motifs found in milled straw lignin (MSL) and cellulase-digested lignin (CEL) isolated from wheat straw by combining quantitative <sup>13</sup>C and HSQC NMR spectral analyses. The results showed that guaiacyl (G) was the predominant unit in wheat straw cell wall lignin over syringyl (S) and hydroxyphenyl (H) units. Up to 8.0 units of tricin were also detected in wheat straw lignin per 100 aromatic rings. Various interunit linkages, including  $\beta$ -O-4,  $\beta$ -5,  $\beta$ - $\beta'$ ,  $\beta$ -1,  $\alpha$ ,  $\beta$ -diaryl ether, and 5-S'/4-O- $\beta'$  as well as potential lignin-carbohydrate complex (LCC) bonds, were identified and quantified. These findings provide useful information for the development of biofuels and lignin-based materials.

**KEYWORDS:** lignin structure, GPC, NMR, lignin-carbohydrate complex, herbaceous crops

## INTRODUCTION

As the second most plentiful polymer found in nature, lignin is deposited at the secondary cell wall and middle lamella, acting as glue to adhere the plant cellular layers together. Lignin is built by three basic structural phenylpropane units: hydroxyphenyl (H), guaiacyl (G), and syringyl (S). The random coupling process between these monolignols will form various interunit linkages, such as arylglycerol- $\beta$ -ether dimer ( $\beta$ -O-4), resinols ( $\beta$ - $\beta'$ ), phenylcoumaran ( $\beta$ -5), spirodienone ( $\beta$ -1), and dibenzodioxin (5-S'/4-O- $\beta'$ ), thereby leading to irregular three-dimensional reticulate structures.<sup>1,2</sup>

The structural integrity of lignin polymers varies by species, subcellular location, and plant tissue.<sup>3</sup> Lignin was commonly defined as woody type lignin and herbaceous crop lignin (grass lignin), respectively. Within woody type plants, gymnosperm (softwood)<sup>4</sup> lignin is composed of only G and H units, whereas angiosperm (hardwood) lignin is composed of G and S units in different proportions.<sup>5</sup> The lignin complex of herbaceous crops, however, contains all three basic units.<sup>1</sup> In addition, for herbaceous lignin hydroxyl groups found at the  $\gamma$ -position of side chains are often esterified by acetate and *p*-coumarate (*p*CA),<sup>6</sup> whereas *p*-hydroxybenzoate (PB) esters were found only in angiosperm lignin.<sup>7</sup> Another important feature that differentiates herbaceous crop lignin from other types of lignin is the linkages that bind lignin to the carbohydrate matrix, which is collectively known as the lignin-carbohydrate complex (LCC). In hardwood and softwood the LCC should contain mostly benzyl ethers (BE) and phenyl glycoside (PhGly) linkages.<sup>8</sup> In herbaceous lignin, on the other hand, ferulate bridges hemicellulose (mainly arabinoxylan) and lignin together to form the LCC.<sup>8</sup>

Given the diversity of lignin substructural motifs, much effort has been made to better determine lignin structures. Traditionally, thermochemical degradation approaches in connection

with gas chromatography and mass spectrometry (GC-MS) have been employed to determine the lignin composition. It has been used in conjunction with different methods such as alkaline nitrobenzene oxidation (NBO), permanganate oxidation, thioacidolysis, derivatization followed by reductive cleavage (DFRC), ozonation, and pyrolysis to try to elucidate lignin structure.<sup>9</sup> Although these methods are successfully applied to analyze specific functional groups, the results obtained often lack global information of lignin structure. In addition, tedious preparation is required for conducting sample analysis with these methods. Spectroscopic methods, which include electronic spectroscopy, vibrational spectroscopy, and nuclear magnetic resonance (NMR), have also been used to determine lignin structure.<sup>10,11</sup> NMR is particularly well suited to probe the lignin structure as it gives structural information at the atomic level and is also able to quantify the substructural motifs within the overall polymer. Utilizing quantitative <sup>13</sup>C NMR analysis of native (not acetylated) and acetylated milled wood lignin, Capanema et al.<sup>4,5</sup> were able to quantify the G and S units as well as other functional groups from softwood (*Picea abies*) and hardwood (*Eucalyptus grandis*). Furthermore, a quick and quantitative 2D HSQC (QQ-HSQC) technique has been developed to allow the assignment of individual signals in crowded spectral regions and to quantitate the various structural units.<sup>12</sup> Individually, these methods are sufficient to assign relatively simple woody lignin; however, for lignin isolated from herbaceous crops, the severe overlap of signals in the aromatic region (mainly caused by the preponderance of ferulate and coumarate), a new approach is needed. Recently, a

**Received:** March 24, 2013

**Revised:** October 13, 2013

**Accepted:** October 16, 2013

**Published:** October 22, 2013

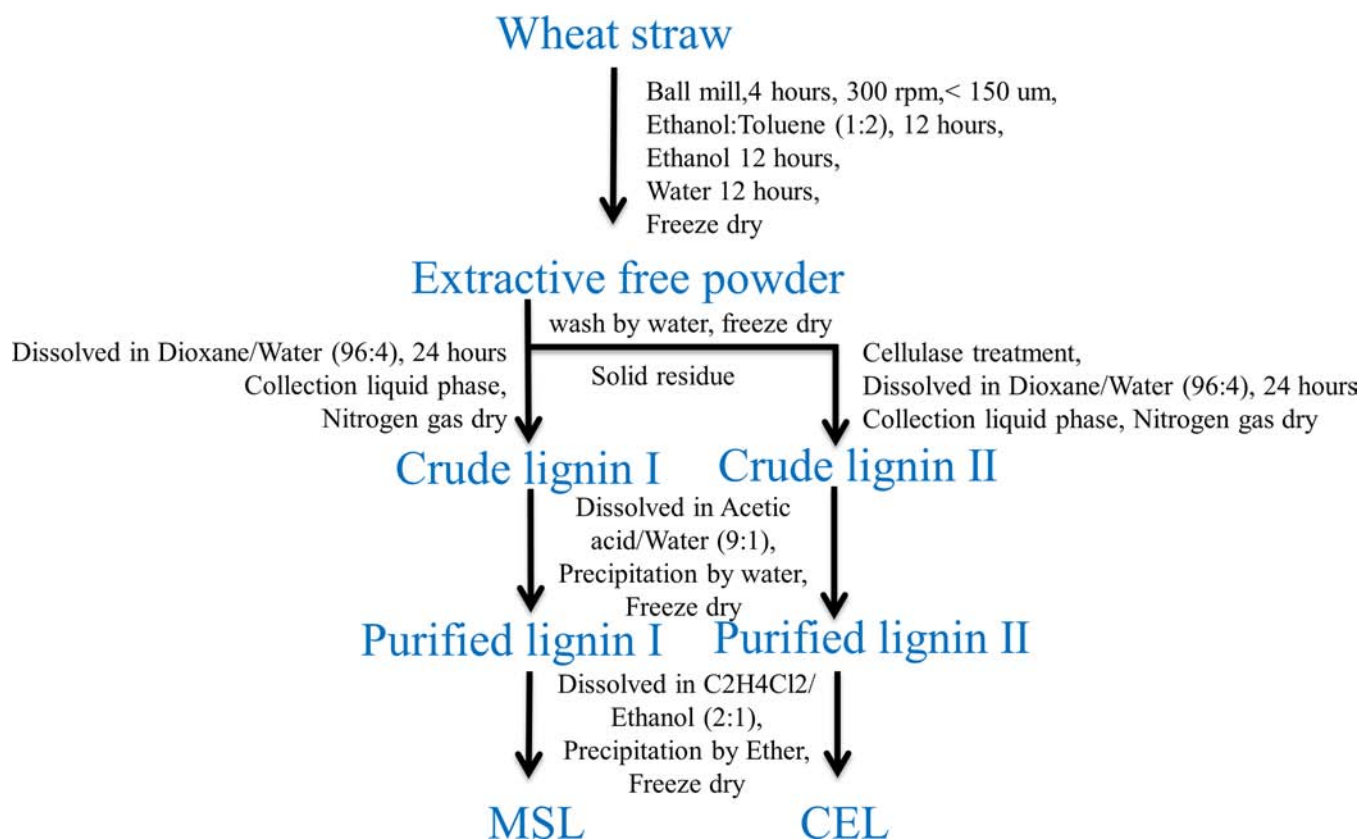


**Figure 1.** Isolation procedures for MSL and CEL from wheat straw.

new combinatorial approach through correlating quantitative  $^{13}\text{C}$  NMR and 2D HSQC NMR has been suggested to take advantage of the spectral dispersion afforded by the 2D spectrum to serve as an internal standard to measure the integral values obtained from the quantitative  $^{13}\text{C}$  spectrum.<sup>13</sup> Selecting the proper internal standard reference signals from the aromatic region, interunit linkage regions, and acylation regions from both  $^{13}\text{C}$  NMR and 2D HSQC NMR spectra can potentially eliminate errors in the quantification of different aromatic units and corresponding side chains<sup>8,13</sup> in herbaceous lignin.

This study aims to develop a quantitative approach to characterize lignin isolated from herbaceous crops. Wheat straw was used as model biomass because structural characteristics of wheat straw lignin have been well investigated and revealed using various NMR analyses.<sup>14–16</sup> Recent research confirmed that *p*-coumarate predominantly acylates the  $\gamma$ -OH of G and S units in wheat straw lignin.<sup>15</sup> A new substructural unit termed triclin was assigned and proposed to link guaiacyl units by  $\beta$ -O-4 linkage.<sup>15</sup> Because lignin preparation methods significantly influence lignin characteristics including structure, cellulase digested lignin (CEL) was isolated along with MSL to comprehensively represent wheat straw lignin in this study. A combined analysis using  $^{13}\text{C}$  NMR and HSQC NMR was established to address the severe overlap of signals in the aromatic region and to reduce error in signal quantification due to differential line widths common in heterogeneous samples such as lignin. This method should also be applicable to the study of various other types of herbaceous crop lignin. Quantitative values of S, G, H, hydroxycinnamates, and triclin units, as well as various types of side-chain substructures and LCC linkages, were estimated. The results suggested that CEL

and MSL had slight but distinguished features for delineating characteristics of wheat straw lignin. CEL contained significantly higher acylation at  $\gamma$ -OH positions and FA compared to MSL. On the other hand, MSL is a better preparation for defining end-groups, spirodienones, and benzyl ether bonds. *p*-Hydroxybenzoate (PB) was detected as one of the hydroxycinnamates in wheat straw.

## ■ MATERIALS AND METHODS

**Lignin Preparation.** Five grams of wheat straw (*Triticum sativum*) (grown in Moscow, ID, USA) was milled (4 h) in a Retsch planetary ball mill PM 100 with zirconium dioxide balls at 300 rpm. The vessel changed rotation sense every 3 min with a 1 min resting step between. The particle size was homogenized by screening through 100 mesh. The well-ground samples were extracted with ethanol/toluene (1:2) for 12 h followed by repeated washings with ethanol and water to remove extractives. The crude lignin (I) was isolated by dioxane/water (96:4, v/v). The residue was subjected to enzymatic hydrolysis in 2% solid loading with 60 FPU/g cellulase and 120 CBU/g glucosidase in 50 mM sodium citrate buffer (pH 5.0) at 50 °C for 72 h. Crude lignin was consequently isolated in dioxane/water solution (96:4, v/v) and purified to (II) cellulase enzymatic lignin (CEL). A scheme illustrating the isolation and purification process is given in Figure 1. Klason lignin content was determined by a two-step acid hydrolysis method.<sup>17</sup> Gel permeation chromatography of the isolated MSL and CEL was performed on a 1260 infinity HPLC system (Agilent Technologies, Santa Clara, CA, USA) using refractive index for detection (RI-G1362A). Three columns were connected in series including PLgel mixed B, PLgel mixed E 5  $\mu\text{m}$  with a pore size of 10000 Å, and PLgel mixed E 5  $\mu\text{m}$  with a pore size of 100 Å (Agilent Technologies). Tetrahydrofuran (THF) was used as the eluent. Molecular weight ranges of the isolated lignin were determined at 25 °C using polystyrene MW standards. CEL had relatively lower solubility (40%)

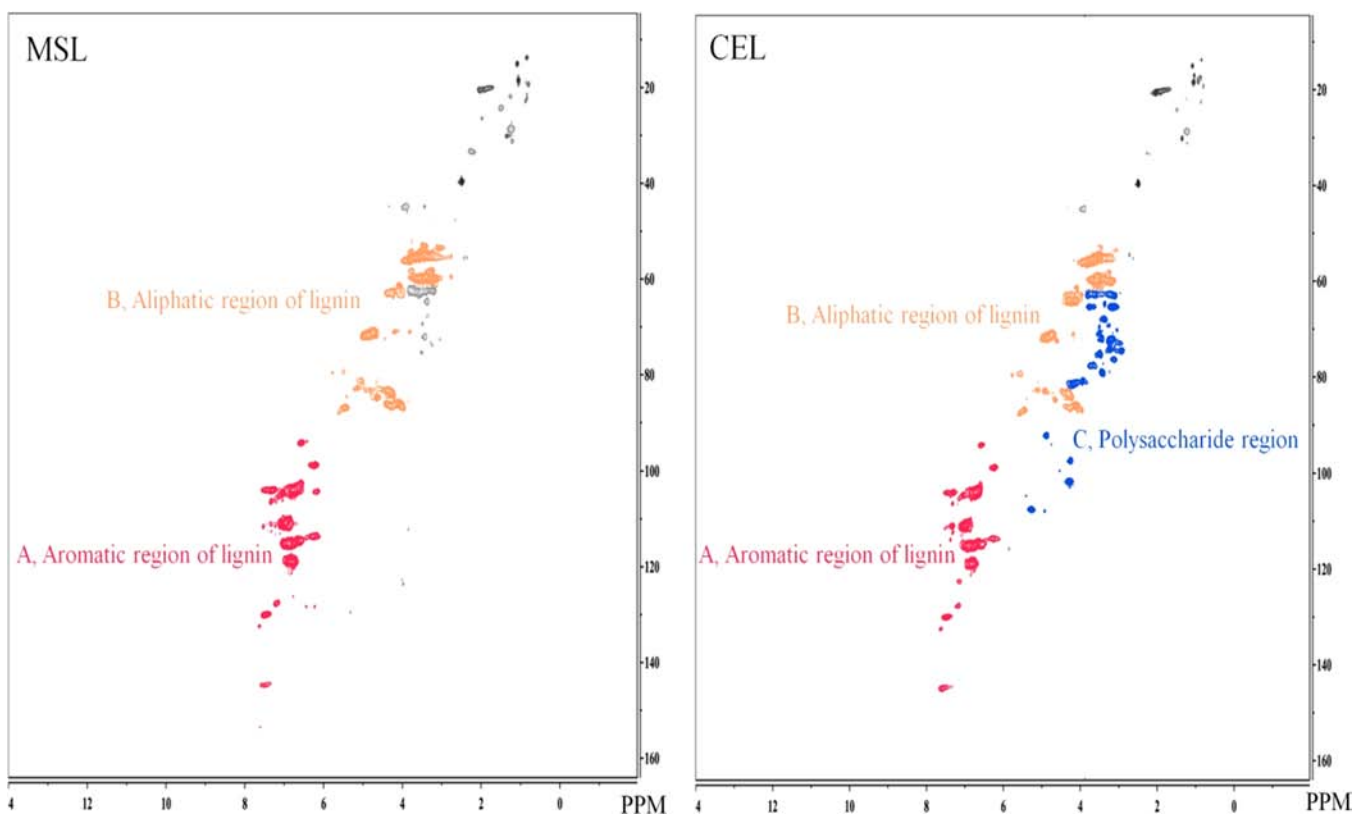


**Figure 2.** Global views of MSL and CEL in HSQC. The red, orange, and blue colors respectively represent (A) the aromatic region of lignin ( $\delta_C/\delta_H$  160–102/8.0–6.0), (B) the aliphatic region of lignin ( $\delta_C/\delta_H$  90–50/6.0–3.0), and (C) the polysaccharide region ( $\delta_C/\delta_H$  110–60/6.0–3.0).

than MSL (100%) in THF solvent and was therefore acetylated according to a previously reported method<sup>15</sup> to increase its solubility.

**NMR Analysis.** NMR spectra were recorded in 99.9% DMSO- $d_6$  plus 0.05% v/v TMS solvent (Cambridge Isotope Laboratories, Inc.) at 300 K on a Varian Inova 500 MHz spectrometer (Agilent Technologies) operating at 499.86 MHz for  $^1\text{H}$  and at 125.7 MHz for  $^{13}\text{C}$ . The residual solvent signal at 2.49 ppm for proton and 39.5 ppm for carbon was used for internal referencing of chemical shifts. For quantitative  $^{13}\text{C}$  NMR, lignin from MSL or CEL was prepared as solutions of 100 mg/mL in DMSO- $d_6$  to which was added 0.01 M chromium(III) acetylacetonate to reduce the  $T_1$  relaxation times of the carbon signals. All spectra were collected using Shigemi microcells with a volume of 250  $\mu\text{L}$ . Carbon spectra were acquired with a sweep width of 26428 Hz using an acquisition time of 0.4 s and a relaxation delay of 2.7 s. A  $90^\circ$  pulse was used for maximum excitation, and broadband  $^1\text{H}$  decoupling was used only during the acquisition time. A total of 22200 scans were recorded for each spectrum, and the FID was apodized with 12 Hz of exponential line broadening prior to zero filling to 65K points and Fourier transformation.  $^1\text{H}$  NMR spectra were recorded at the same concentration of lignin without chromium(III) acetylacetonate using a sweep width of 7500 Hz. An acquisition time of 1.9 s and a relaxation delay of 3.5 s were used to collect 64 scans for each spectrum. The FID was apodized with 0.5 Hz of exponential line broadening prior to zero filling to 65K points and Fourier transformation. HSQC spectra were acquired using the pulsed field gradient coherence selection and using spectral editing to allow for discrimination of methyl and methine signals from those of methylene signals. Spectral widths of 8000 and 20100 Hz were used for the  $^1\text{H}$  and  $^{13}\text{C}$  dimensions, respectively. An acquisition time of 0.06 s was used for directly observing dimension, and an acquisition time of 0.0127 s was used for the indirect dimension. A one-bond  $^1\text{H}$ - $^{13}\text{C}$   $J$  coupling of 140 Hz was used and a total of  $2 \times 256$  increments in  $t_1$  were acquired using the gradient echo-antiecho selection technique for pure phase line shape in F1. The FIDs were zero-filled once to 2048 points in  $t_2$  and apodized with a Gaussian

function prior to Fourier transformation. Data in  $t_1$  were extended by a factor of 2 with linear prediction followed by zero filling to 2K points, apodizing with a Gaussian function, and Fourier transformation. The system has been used for analysis of various treated samples of wheat straw lignin and checked with model compounds. Interactive integrations of peaks in the  $^{13}\text{C}$  / $^1\text{H}$  spectrum and contours in 2D HSQC plots were measured using MestReNova software.

## RESULTS AND DISCUSSION

**Characteristics of CEL and MSL.** Figure 2 shows the full HSQC spectra of MSL and CEL isolated from wheat straw. Chemical shift assignments of various lignin moieties have been reported in several previous studies.<sup>4,15,18,19</sup> Typically, three main regions in HSQC NMR spectra of lignocellulosic samples are observed: the aromatic region of lignin ( $\delta_C/\delta_H$  160–102/8.0–6.0), the aliphatic region of lignin (main interunits ranged from  $\delta_C/\delta_H$  90–50/6.0–3.0, but some signals extend farther upfield than 3 ppm), and the polysaccharide anomeric region ( $\delta_C/\delta_H$  110–60/6.0–3.0). In the aromatic region,  $^{13}\text{C}$ - $^1\text{H}$  correlations from aromatic rings such as S 2/6, G 2, and H 2/6 as well as other hydroxycinnamic compounds can be observed. The interunits of lignin including  $\beta$ -O-4,  $\beta$ -5,  $\beta$ - $\beta'$ ,  $\beta$ -1, and 5-5'/4-O- $\beta'$  are found in the aliphatic regions of the HSQC spectrum.

Various signals from polysaccharides have been detected in CEL (Figure 2), providing information on what types of polysaccharide polymers may be involved in LCC construction. The peaks of  $\beta$ -D-xylopyranoside were found in the ranges of  $\delta_C/\delta_H$  85–60/4.5–2.5, 97/4.1, and 102/4.3.<sup>18</sup> Moreover, correlations from  $\alpha$ -D-xylopyranoside and  $\alpha$ -L-arabinofuranoside were at  $\delta_C/\delta_H$  92/4.9 and 108/4.9, respectively.<sup>18</sup> Due to degeneracy of chemical shifts in polysaccharides it is often

Table 1. Chemical Composition of Wheat Straw Samples and Molecular Weight and Yield of MSL and CEL<sup>a</sup>

|                               | glucan (%)   | xylan (%)    | arabinan (%) | galactan (%) | lignin <sup>b</sup> (%) | molecular weight (g/mol) |                   | yield (%)    |
|-------------------------------|--------------|--------------|--------------|--------------|-------------------------|--------------------------|-------------------|--------------|
|                               |              |              |              |              |                         | M <sub>n</sub>           | M <sub>w</sub>    |              |
| raw wheat straw               | 52.46 ± 1.08 | 17.95 ± 0.59 | 2.75 ± 0.12  | 0.62 ± 0.01  | 18.52 ± 0.22            |                          |                   |              |
| cellulase treated wheat straw | 34.67 ± 3.11 | 13.77 ± 1.72 | 0.64 ± 0.51  | 0.14 ± 0.22  | 35.7 ± 2.06             |                          |                   |              |
| MSL                           |              |              |              |              | 97                      | 2026                     | 3457              | 14.05 ± 0.78 |
| CEL                           |              |              |              |              | 90                      | 1177                     | 3228              | 26.48 ± 1.66 |
|                               |              |              |              |              |                         | 3789 <sup>c</sup>        | 7774 <sup>c</sup> |              |

<sup>a</sup>Data presented triplicate experiments. <sup>b</sup>Acid-insoluble lignin and acid-soluble lignin. <sup>c</sup>Molecular weight of acetylated CEL.

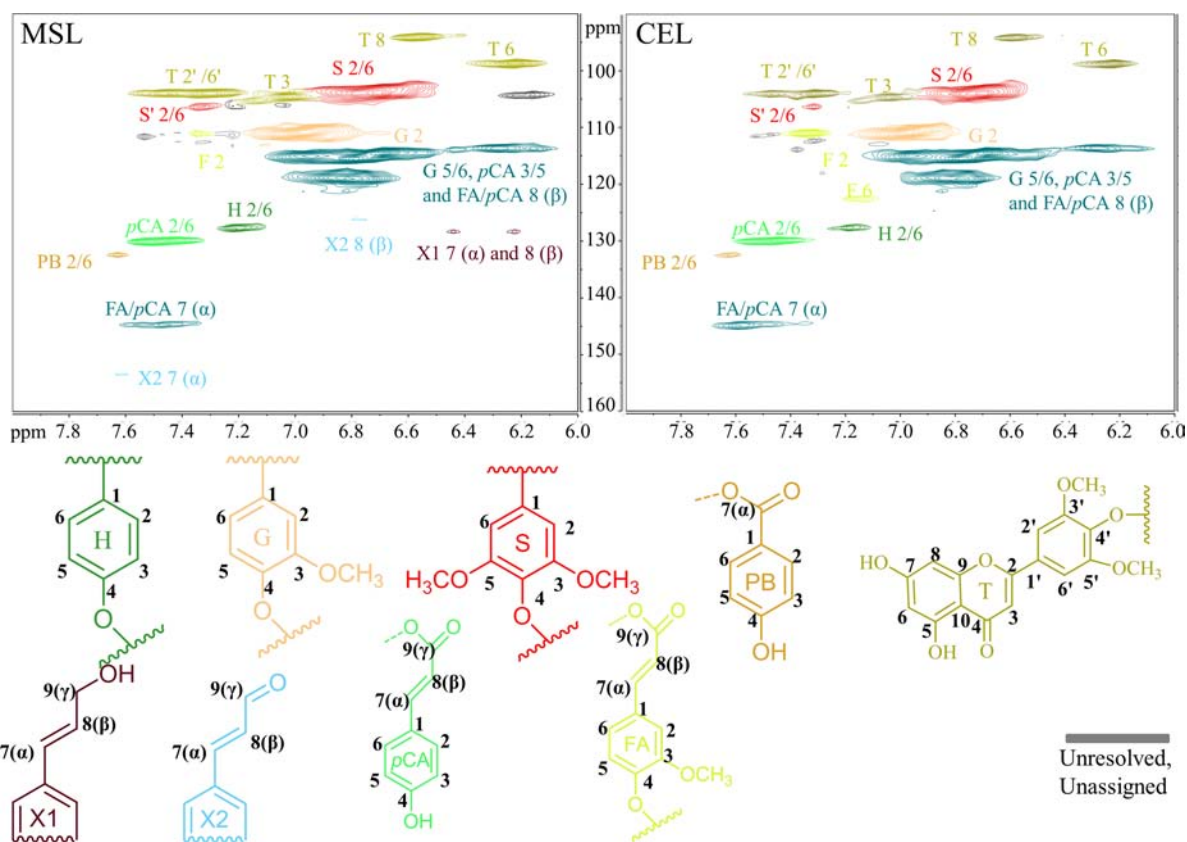


Figure 3. Aromatic regions in HSQC spectra of MSL and CEL isolated from wheat straw.

difficult to make specific assignments. In addition, the longer relaxation times for the polysaccharide signals compared to other structural moieties resulted in relatively high intensity in the HSQC spectra.<sup>4</sup> Quantification of carbohydrates associated with the isolated lignin samples is not discussed in this paper. Compared to MSL, a significantly higher amount of polysaccharides was detected in the CEL spectrum. This result was further verified by chemical composition analysis, which indicated that the CEL was composed of 90% Klason lignin compared to 97% Klason lignin in MSL. The molecular weight and yield of MSL and CEL are shown in Table 1. The MSL had a relatively lower yield (14%) compared to the yield of CEL (26%) when based on the calculated Klason lignin content of raw wheat straw. It should be noted that the preparation procedure may have altered the structure of native lignin; therefore, structural information provided by MSL and CEL can be considered only as references for predicting native lignin structure.

**Lignin Quantification Process by Combination of <sup>13</sup>C NMR and HSQC NMR.** The quantity of specific compounds

was expressed as number per aromatic ring (Ar) or number per 100 aromatic rings (100 Ar). The integral of the resonances between 160 and 102 ppm in the quantitative <sup>13</sup>C NMR has been assumed to contain the total carbon atoms from all aromatic rings within the lignin. Logically, an aromatic ring contributes six carbons; however, the signals of  $\alpha$ - and  $\beta$ -positions of the vinyl group in ferulate (FA), *p*-coumarate (*p*CA), cinnamyl alcohol (X1), and cinnamyl aldehyde (X2) also occur in the aromatic region and interfere with the overall analysis. Their proportional distribution in lignin polymers varies by species. In woody type of lignin, the main interference comes from end groups of lignin such as X1 and X2, which generally contributed 0.12 vinylic carbon to every aromatic ring.<sup>4</sup> Herbaceous lignin, on the other hand, contains a greater amount of vinylic carbons. Figure 3 shows the aromatic regions of HSQC spectra in MSL and CEL isolated from the wheat straw. It is clear that wheat straw lignin contains FA, *p*CA, and PB, along with lignin end groups (X1 and X2). T3 from triclin overlapping the syringyl unit signals has also been recently reported.<sup>15</sup> To calculate the aromatic rings in herbaceous lignin

**Table 2. Quantification of Aromatic Moieties (Lignin, Cinnamates, Lignin End Group, and Lignin) by Combination Analysis of  $^{13}\text{C}$  and HSQC NMR Spectra of Wheat Straw Isolated MWL and CEL**

| aromatic moiety                    | $\delta_{\text{C}}/\delta_{\text{H}}$ and assignments                                   | MWL             |                | CEL             |                |
|------------------------------------|---|-----------------|----------------|-----------------|----------------|
|                                    |   | Ar <sup>a</sup> | % <sup>b</sup> | Ar <sup>a</sup> | % <sup>b</sup> |
| <b>lignin aromatic units</b>       |   |                 |                |                 |                |
| syringyl                           | 103.9/6.7 (S2/6), 106.4/7.4 (S'2/6 with $\alpha$ oxidation)                             | 25.7            | 37.5           | 27.3            | 40.1           |
| guaiacyl                           | 110.8/6.97 (G2), 115.0/6.94 (G5), 118.9/6.81 (G6)                                       | 41.2            | 60.2           | 39.3            | 57.8           |
| <i>p</i> -hydroxyphenyl            | 127.7/7.21 (H2/6)   | 1.6             | 2.3            | 1.4             | 2.1            |
| S/G ratio                          |   | 0.63            |                | 0.69            |                |
| <b>hydroxycinnamates</b>           |   |                 |                |                 |                |
| <i>p</i> -benzoates                | 132.4/7.63 (PB2/6)  | 0.5             | 0.7            | 1.2             | 1.8            |
| <i>p</i> -coumarate                | 130.0/7.47 ( <i>p</i> CA2/6), 115.5/6.79 ( <i>p</i> CA3/5), 144.74/7.47 ( <i>p</i> CA7) | 5.4             | 7.9            | 5.5             | 8.1            |
| ferulate                           | 110.9/7.32 (FA2), 122.5/7.15 (FA6)  | 0.6             | 0.9            | 6.4             | 9.4            |
| <i>p</i> -coumarate/ferulate ratio |   | 9               |                | 0.86            |                |
| cinnamates/lignin ratio            |   | 0.09            |                | 0.23            |                |
| <b>lignin end group</b>            |   |                 |                |                 |                |
| cinnamyl aldehyde                  | 153.5/7.62 (X2 $\alpha$ ), 126.2/6.78 (X2 $\beta$ )                                     | 0.1             | 0.1            | ND              |                |
| cinnamyl alcohol                   | 128.34/6.44 (X1 $\alpha$ ), 128.35/6.22 (X1 $\beta$ )                                   | 0.6             | 0.9            | ND              |                |
| <b>lignan</b>                      |   |                 |                |                 |                |
| tricin                             | 104.04/7.30 (T2'/6'), 104.65/7.03 (T3), 94.1/6.56 (T8), 98.8/6.22 (T6)                  | 8.5             | 12.4           | 5.6             | 8.2            |

<sup>a</sup>Amount of specific interunit linkage was expressed as number per 100 Ar. <sup>b</sup>Amount of specific interunit linkage was expressed as percentage of S + G + H.

samples, the number of vinylic carbons was quantified using the following equation:

$$\frac{\text{vinylic carbons}}{6} = \frac{(I_{\text{FA}7} + I_{\text{pCA}7} + I_{\text{X}1\alpha} + I_{\text{X}2\alpha} + I_{\text{T}3}) \times 2}{\frac{I_{\text{S}2/6} + I_{\text{H}2/6} + I_{\text{pCA}2/6} + I_{\text{T}2'/6'}}{2} + I_{\text{G}2} + I_{\text{F}2}} \quad (1)$$

In this equation, the signal of each aromatic unit was identified and integrated in the HSQC spectra. The total carbons per aromatic ring in the aromatic region are equal to vinylic carbons plus six. With this relationship, values for MSL and CEL were derived as 6.25 and 6.28 carbons per aromatic ring (carbons/Ar), respectively, which subsequently were used to quantify the number of aromatic ring (Ar) by dividing the integral of the 160–102 ppm region of the quantitative  $^{13}\text{C}$  NMR by the corresponding carbons/Ar ratio. However, in the case of CEL sample, signals corresponding to carbohydrates were also detected in the 160–102 ppm region (Figure 2). To exclude the interference of partially overlapping carbohydrates in the aromatic region, the total integral of CEL was corrected by correlating the integration of the carbohydrate crosspeaks to the total aromatic region's integration in HSQC spectra. However, it may therefore underestimate total aromatic rings in CEL because intensities from carbohydrate might be over-presenting in HSQC spectra.

The second step to quantify herbaceous lignin units is selection of internal reference signals that (1) are easily identifiable in both  $^{13}\text{C}$  and HSQC spectra, (2) are predominant in lignin polymers, and (3) can be used to eliminate errors caused by heterogeneity of polymer in specific region. In this study, three regions of  $^{13}\text{C}$ – $^1\text{H}$  correlations,  $\delta_{\text{C}}/\delta_{\text{H}}$  113–109/7.6–6.8,  $\delta_{\text{C}}/\delta_{\text{H}}$  88–82/5.6–3.9, and  $\delta_{\text{C}}/\delta_{\text{H}}$  66–58/4.5–3.0, were chosen as internal references to transform specific lignin unit's integration into quantitative values. Zhang and Gellerstedt<sup>13</sup> illustrated that the selection of these specific regions as internal standard clusters to quantify individual signals in HSQC spectra can effectively avoid complications arising from  $T_2$  relaxation, resonance offsets, coupling constant deviations, and homonuclear couplings. It needs to be pointed

out that a major assumption has been made that the level of intensities of aromatic and aliphatic resonances attributed to different lignin structures in the HSQC spectra are comparable and compatible to the same signals from the quantitative  $^{13}\text{C}$  NMR spectra.

**Analysis of Lignin Aromatic Components.** Figure 3 indicates that wheat straw cell walls were mainly enriched with G and S units along with a minor amount of hydroxyphenyl units. The detailed assignments and amounts of G, S, and H in MSL and CEL have been summarized in Table 2. For quantification of the aromatic region, the range of  $\delta_{\text{C}}/\delta_{\text{H}}$  113–109/7.6–6.8 was used as internal standard. The  $^{13}\text{C}$ – $^1\text{H}$  correlation for S2/6 was at  $\delta_{\text{C}}/\delta_{\text{H}}$  104.0/6.70, except  $\alpha$ -oxidized S2/6 shifted to  $\delta_{\text{C}}/\delta_{\text{H}}$  106.4/7.4. The correlations of G2 units were found at  $\delta_{\text{C}}/\delta_{\text{H}}$  110.8/6.97 and were used to represent all G aromatic rings as previously reported.<sup>18</sup> The signals from the G5 and G6 positions overlapped at  $\delta_{\text{C}}/\delta_{\text{H}}$  115.0/6.94 and  $\delta_{\text{C}}/\delta_{\text{H}}$  118.9/6.81 in the HSQC spectra.<sup>18</sup> The resonance from H2/6 was barely observed at  $\delta_{\text{C}}/\delta_{\text{H}}$  127.7/7.21. The integration values of S2/6 or H2/6 crosspeaks in the HSQC needed to be divided by 2. The same approach was applied to quantify *p*CA, triclin, and  $\beta$ - $\beta'$ . The quantification results showed that MSL and CEL isolated from wheat straw shared a similar distribution of H units but differed for G and S units. The change of G and S lignin in MSL and CEL resulted in increasing S/G ratio from 0.63 for MSL to 0.69 for CEL. Zhou et al.<sup>20</sup> reported the distribution of S and G lignins in the cell wall of *Populus trichocarpa* by a combination of Bi ToF-SIMS spectral image acquisition and  $\text{C}_{60}$  sputtering, demonstrating that G lignin was preferentially located in the middle lamella in contrast to S lignin, which was preferentially located in the inner cell wall area. The difference in G lignin content suggests that MSL tends to represent the lignin from the middle lamella, whereas CEL represents lignin from the secondary cell wall. Special attention was paid to the relatively lower S/G ratio in both MSL and CEL. It was thought, on the basis of wet chemical methods, that wheat straw lignin contained even amounts of S and G units.<sup>21,22</sup> However, NMR analysis<sup>14,15</sup> revealed that lignin from wheat straw was dominated by G units. Such a

**Table 3. Quantification Analysis of Aliphatic Region ( $\beta$ -O-4,  $\beta$ - $\beta$ ,  $\beta$ -5,  $\beta$ -1, D, F, and LCC Bondings) by Combination Analysis of  $^{13}\text{C}$  and HSQC NMR Spectra of Wheat Straw Isolated MWL and CEL**

| aliphatic region                    | $\delta_{\text{C}}/\delta_{\text{H}}$               | MWL             |                | CEL             |                |
|-------------------------------------|---|-----------------|----------------|-----------------|----------------|
|                                     |   | Ar <sup>a</sup> | % <sup>b</sup> | Ar <sup>a</sup> | % <sup>b</sup> |
| <b>interunit bondings</b>           |   |                 |                |                 |                |
| $\alpha$ -OH/ $\beta$ -O-4          | 71.1/4.74 (A $\alpha$ -G), 71.8/4.8 (A $\alpha$ -S) | 28.3            | 75.3           | 33.8            | 72.0           |
| $\alpha$ -keto/ $\beta$ -O-4        | 82.7/5.1 (A $\alpha$ -keto)                         | 1.5             | 4.0            | 2.4             | 5.2            |
| <b>total <math>\beta</math>-O-4</b> |   | 29.8            | 79.3           | 36.5            | 77.1           |
| phenylcoumaran                      | 85.9/5.5 (B $\alpha$ ), 53.0/3.4 (B $\beta$ )       | 5.4             | 14.4           | 5.7             | 13.3           |
| resinols                            | 84.8/4.7 (C $\alpha$ ), 53.5/3.1 (C $\beta$ )       | 1.3             | 3.5            | 0.9             | 1.9            |
| dibenzodioxocin                     | 83.4/4.9(D $\alpha$ ), 85.5/3.8 (D $\beta$ )        | 0.2             | 0.5            | 2.0             | 4.3            |
| spirodienones                       | 81.4/5.0 (E $\alpha$ ), 59.5/2.8 (E $\beta$ )       | 0.4             | 1.1            | ND              | ND             |
| $\alpha,\beta$ -diaryl ether        | 79.6/5.5 (F $\alpha$ )                              | 0.5             | 1.2            | 2.1             | 4.6            |
| <b>total side chains</b>            |   | 37.6            | 100            | 47.0            | 100            |
| <b>LCC bondings</b>                 |   |                 |                |                 |                |
| phenyl glycoside                    | 103–96/5.2–4.8                                      | ND              |                | ND              |                |
| benzyl ethers C <sub>1</sub>        | 81/4.6  | 0.3             |                | ND              |                |
| benzyl ethers C <sub>2</sub>        | 81/5.0  | 1.5             |                | ND              |                |

<sup>a</sup>Amount of specific interunit linkage was expressed as number per 100 Ar. <sup>b</sup>Amount of specific interunit linkage was expressed as percentage of total side chains.

composition was similar to that of flax straw.<sup>23,24</sup> This suggests that 2D NMR may have advantages over traditional methods for delineating lignin composition. Because deposition of S lignin in the secondary cell wall played an important role in the maturation of angiosperm cell walls, the lower content of S lignin in wheat straw cell wall indicated a different regulation of the lignification process in xylem.<sup>25</sup>

Near the S 2/6 signal, several  $^{13}\text{C}$ – $^1\text{H}$  correlations of tricrin were identified at  $\delta_{\text{C}}/\delta_{\text{H}}$  94.1/6.56 (T8),  $\delta_{\text{C}}/\delta_{\text{H}}$  98.8/6.22 (T6),  $\delta_{\text{C}}/\delta_{\text{H}}$  104.04/7.30 (T 2'/6'), and  $\delta_{\text{C}}/\delta_{\text{H}}$  104.65/7.03 (T3) (Figure 3).<sup>15</sup> As one type of flavonoid, tricrin is generally found in most cereal crop plants in both free and conjugated forms, which function as antioxidants, antimicrobial/antiviral agents, allelochemicals, photoreceptors, visual attractors, and signaling molecules in plant growth and development.<sup>25</sup> A recent study suggested that tricrin may be an important phenolic brick in the building of the herbaceous lignin complex.<sup>15</sup> The observance of a correlation of C4 in tricrin and the  $\beta$  proton in a G unit demonstrated that tricrin was incorporated into lignin via a  $\beta$ -O-4 linkage.<sup>15</sup> Therefore, it is necessary to quantify the tricrin content in herbaceous lignin samples; in this case, the integration of T3 and T 2'/6' was selected to represent tricrin content. The results showed that tricrin was relatively rich in MWL (8.5 per 100 Ar) compared to its content in CEL (5.6 per 100 Ar) (Table 2). The decrease of tricrin in CEL may be related to the reduction of G units. The high proportion of tricrin in wheat straw cell wall provides a new insight into herbaceous lignin composition.

The crosspeak at  $\delta_{\text{C}}/\delta_{\text{H}}$  130.0/7.47 in HSQC spectra was assigned to the 2- and 6-positions of *p*-coumarate (*p*CA), whereas the crosspeak of *p*CA 3/5 at 115.5/6.79 ppm was severely overlapped with the signal of G 5/6. Integration of *p*CA 2/6 was used for the quantification of *p*CA content. The results showed that MSL and CEL contained approximately 5.5 *p*CA per 100 Ar, which was consistent with previous results on wheat straw (with 4% with respect to total lignin).<sup>15,26</sup> *p*CA has been reported to acylate at  $\gamma$ -OH by ester bonds in various herbaceous crops via lignification of *p*-coumaroylated monolignols.<sup>27</sup> The preferential acylation of syringyl units versus guaiacyl units by *p*CA was found in maize lignin and bamboo lignin,<sup>28</sup> revealing its potential role in transferring radical to

synapyl alcohol for incorporation in late cell wall formation.<sup>29</sup> However, in wheat straw, *p*CA acylating lignin monomers with  $\beta$ -ether structure was not detected; thus, a new hypothesis for lignification was proposed: coniferyl *p*CA rather than sinapyl *p*CA was favored during early cell wall development.<sup>15</sup> Besides *p*CA, the crosspeak at  $\delta_{\text{C}}/\delta_{\text{H}}$  132.4/7.65 was assigned to PB2/6 and was identified in both MSL and CEL. PB is generally found in angiosperm lignin including aspen, oil palm, poplar, and willows.<sup>10</sup> Similar to *p*CA, PB acylated the  $\gamma$ -OH of lignin side chains via lignification of *p*-hydroxybenzoylated lignin monomers.<sup>18</sup> Although only a minor amount of PB was detected (Table 2), it implied that herbaceous crops, at least wheat straw, were also partially acylated by PB that may take part in lignification at the early stage of cell wall development. In addition, signals from side chains of cinnamyl alcohol end groups (X1) and cinnamyl aldehyde end groups (X2) appeared at  $\delta_{\text{C}}/\delta_{\text{H}}$  128.3/6.44 (X1 $\alpha$ ), 128.3/6.22 (X1 $\beta$ ), 153.5/7.62 (X2 $\alpha$ ), and 126.2/6.78 (X2 $\beta$ ) in MSL, respectively. The occurrence of end groups in lignin is formed primarily from endwise coupling of monolignols with the growing lignin polymer.<sup>10</sup> The integration of  $\beta$ -position crosspeaks was used to quantify their amounts. It showed that MSL contained 0.6 X1 (per 100 Ar) and 0.1 X2 (per 100 Ar).

Ferulate (FA) is the hydroxycinnamate that is mainly involved in lignin–polysaccharide cross-linking. Both ferulate and its dehydromers extensively acylate the C5-OH position of arabinoxylans by ester bonding and act as initiation sites for incorporation into lignin complex through forming  $\beta$ -X, 4-O-X, or 5-X structures with monolignols.<sup>30–32</sup> In HSQC spectra, the FA2 correlation was at  $\delta_{\text{C}}/\delta_{\text{H}}$  110.9/7.32, and its 6-position correlation appeared at  $\delta_{\text{C}}/\delta_{\text{H}}$  112.5/7.15. The crosspeaks of FA5, FA7, and FA8, however, were either partially resolved or overlapped with other signals.<sup>18</sup> Thus, the integration of the FA2 crosspeak was used for quantitation. Table 2 shows the differences between MSL and CEL with respect to FA content. The CEL had higher amounts of FA than MSL, reaching 6.4 units per 100 Ar. The absence of FA in MSL of wheat straw demonstrated that FA was not acylated by  $\gamma$ -esters. Because FA is an important component for forming the lignin–carbohydrate complex, the variation can reflect the changes of LCC in herbaceous lignin. The quantitative results further suggest that

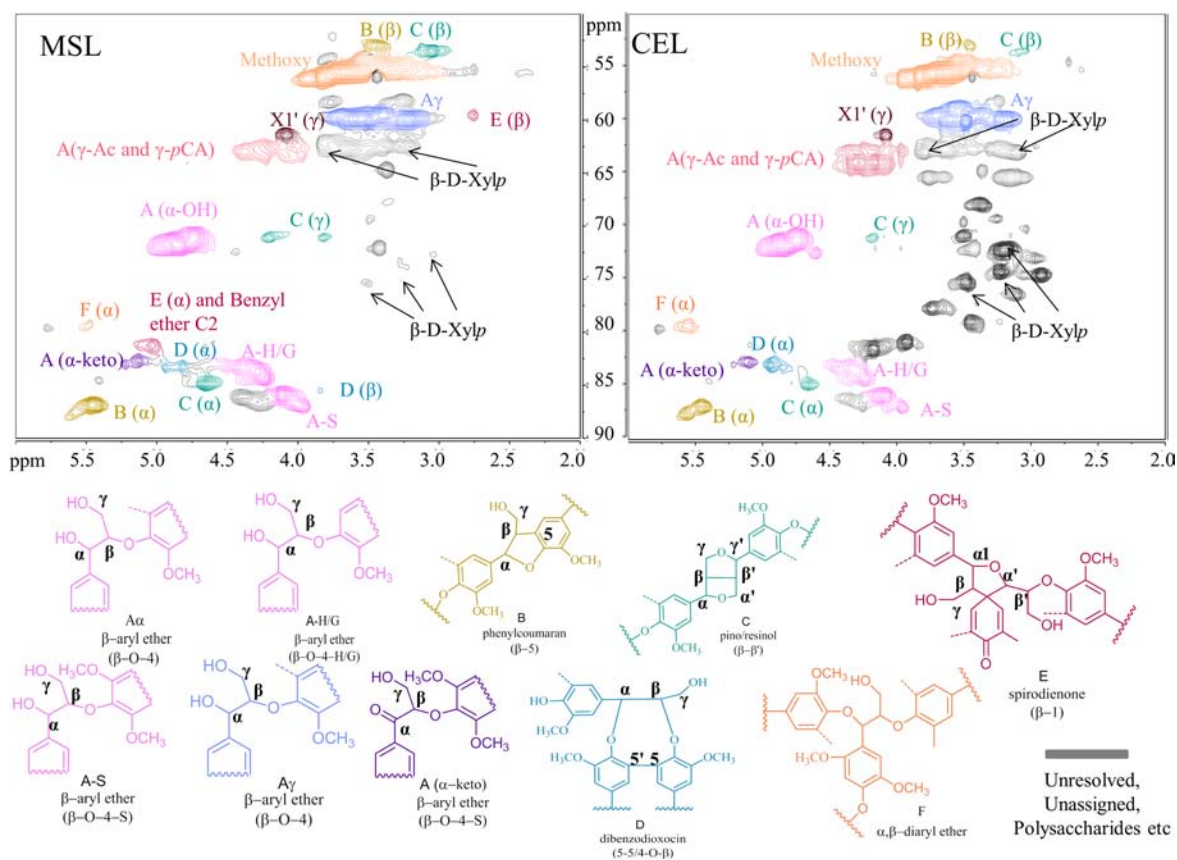


Figure 4. Aliphatic regions of MSL and CEL isolated from wheat straw in HSQC spectra.

preparation of CEL is critical for evaluating FA content in lignin.

**Analysis of Lignin Side Chains.** Table 3 summarizes the quantitative amounts and/or relative abundances of main side-chain types in lignin, including  $\beta$ -O-4,  $\beta$ -5,  $\beta$ - $\beta'$ ,  $\beta$ -1, and 5-5'/4-O- $\beta'$  as well as LCC bondings. To eliminate error from variation of  $^1J_{C-H}$ , the  $\delta_C/\delta_H$  88–82/5.6–3.9 region was used to normalize each interunit. The crosspeaks corresponding to the  $\alpha/\beta$ -position linked with  $\beta$ -O-4 structure were widely distributed in the aliphatic region. The signals of  $\delta_C/\delta_H$  71.1/4.74 and 71.8/4.8 were ascribed to the  $\alpha$ -OH position ( $A\alpha$ -OH) attached to G and S units by  $\beta$ -O-4 structures. The signals from the  $\beta$ -position ( $A$ -H/G, S) were found in the range of  $\delta_C/\delta_H$  82–88/4.5–3.9, but the  $\alpha$  oxidation structure ( $A\alpha$ -keto) was shifted to  $\delta_C/\delta_H$  82.7/5.1 (Figure 4). Compared with the quantitative values of  $\alpha$ - and  $\beta$ -positions in the  $\beta$ -O-4 structure, the results from total  $\beta$ -position were always lower than the corresponding value from the  $\alpha$ -position in both MSL and CEL (Table 3). This may result from oxidation that took place at the  $\beta$ -position during the ball-milling process. Thus, the crosspeaks of  $A\alpha$ -OH and  $A\alpha$ -keto in HSQC spectra was used to represent total  $\beta$ -O-4 linkages.  $\beta$ -O-4 linkage was the dominant interunit in gymnosperms,<sup>4</sup> angiosperms,<sup>5</sup> and herbaceous crops<sup>1</sup> and acted as a vital indicator to reflect the lignin complex's intactness. Unlike its higher content in woody samples,<sup>4,5</sup> the lower amount of  $\beta$ -O-4 in wheat straw suggests relatively more guaiacyl units involved in the construction of non- $\beta$ -O-4 dimers.<sup>33</sup>

Phenylcoumaran (B) was the second most abundant interunit ( $\beta$ -5) in wheat straw. Apparently, the G unit was the main building block again for this structure by coupling its

available 5-position with monolignol's  $\beta$ -positions. The crosspeaks found at  $\delta_C/\delta_H$  85.9/5.5 and  $\delta_C/\delta_H$  53.0/3.4 were attributed to  $\alpha$  and  $\beta$  substructures, respectively. Consistent with the existence of higher amount of G units rather than S units in wheat straw, it was estimated that up to 14% (approximately 5.4 units per 100 Ar) of total side chains was made of  $\beta$ -5 structures which explains the relatively lower  $\beta$ -O-4 interunits compared to syringyl-rich angiosperms or grasses.

Along with  $\beta$ -O-4 and  $\beta$ -5 interunits, resinols (C) with  $\beta$ - $\beta'$  structure were observed at  $\delta_C/\delta_H$  84.8/4.7 ( $C\alpha$ ) and  $\delta_C/\delta_H$  53.5/3.1 ( $C\beta$ ). The crosspeaks at  $\delta_C/\delta_H$  71.5/4.2 and  $\delta_C/\delta_H$  71.5/3.8 were ascribed to its  $\gamma$ -position. Unlike  $\beta$ -5 interunits,  $\beta$ - $\beta'$  was favored in syringyl-rich lignin due probably to the higher stability and longer lifetimes of the sinapyl alcohol radicals.<sup>10</sup> In MSL and CEL, the values of C units were 1.3 and 0.9 per 100 Ar, respectively, which confirmed the preference for syringyl units. It is also worth noting that acylated ferulate can couple with either sinapyl alcohol or coniferyl alcohol to form  $\beta$ - $\beta'$  structures.<sup>31</sup>

Minor amounts of dibenzodioxocin (D), spirodienone (E), and  $\alpha,\beta$ -diaryl ether (F) were present in wheat straw lignin. The  $\alpha$ -position of dibenzodioxocin (D) was observed at  $\delta_C/\delta_H$  83.4/4.9; however, only weak crosspeaks for  $\beta$  were observed at  $\delta_C/\delta_H$  85.5/3.8 in MSL. The D structure arose from a coupling reaction between monolignols and 5-5' units.<sup>34</sup> The incidence of D structure largely depended on G units; syringyl-rich lignin generally contained very low levels of D structure.<sup>10</sup> In this study, up to 1.8 D units per 100 Ar was detected in CEL, which was about 4% of total side chains. Spirodienone (E) structure was detected with NMR in spruce, birch, kenaf, cortex, and elephant grass, almost in all plant lignin.<sup>6,35</sup> The occurrence

of  $\beta$ -1 structures after acidolytic treatment resulted from the degradation of E structures.<sup>10</sup> The  $\beta$ -position of E was observed at  $\delta_C/\delta_H$  85.5/3.8 in MSL, suggesting the better representation in MSL than in CEL. The amount of E in wheat straw lignin was estimated to be 0.4 unit per 100 Ar. With respect to  $\alpha,\beta$ -diaryl ether (F), the peak of  $\delta_C/\delta_H$  79.6/5.5 was assigned to the  $\alpha$ -position.<sup>6,14,15</sup> The quantification results showed that CEL presented more F units (2.1 units per 100 Ar) than in MSL (0.5 unit per 100 Ar).

Special attention was paid to the evaluation of potential LCC in wheat straw lignin as the LCC is correlated with the recalcitrance of lignocellulosic biomass. There were four possible LCC linkages to bridge carbohydrate to lignin: phenyl glycoside, benzyl ether,  $\gamma$ -ester, and hydroxycinnamate-related linkages. The former three linkages are the predominant LCC bonds in woody lignin.<sup>8</sup> No detectable signals was found in the range of  $\delta_C/\delta_H$  103–96/5.2–4.8 (Figure 4), which was ascribed to carbohydrate C-1 correlation in phenyl glycoside structure.<sup>8</sup> However, the peaks from benzyl ethers were indeed observed at  $\delta_C/\delta_H$  81/4.6 (benzyl ethers C<sub>1</sub>) and 81/5.0 (benzyl ether C<sub>2</sub>) in HSQC spectra of MSL, which were not detected in CEL. Benzyl ethers C<sub>1</sub> referred to linkages between the  $\alpha$ -position of lignin and primary OH groups of carbohydrate, whereas the linkages attached to secondary OH groups of carbohydrates belonged to benzyl ethers C<sub>2</sub>.<sup>8</sup> Due to the fact that benzyl ether C<sub>2</sub> partially overlapped with the signal from the  $\alpha$ -position of E structures, the quantitative value needed to be corrected for the interference of E. The quantitative results indicated that MSL contained 5 times as much benzyl ether C<sub>2</sub> (1.5 per 100 Ar) over benzyl ether C<sub>1</sub> (0.3 per 100 Ar). The higher existence of benzyl ether C<sub>2</sub> demonstrated that xylan was the major carbohydrate attached to the  $\alpha$ -position of lignin side chains. Although a great amount of  $\gamma$ -acylation appeared in the range of  $\delta_C/\delta_H$  65–62/4.5–4, it was not feasible to assign this type of LCC to  $\gamma$ -ester linkages. It has been proven that herbaceous lignin was largely acylated by *p*CA and acetate in wheat straw.<sup>6,15</sup> Although *p*CA may relate to carbohydrate, in most cases, *p*CA persevered as a free phenolic compound in herbaceous lignin.<sup>6,15</sup> It is possible to conclude that the existence of  $\gamma$ -ester LCC will be limited in wheat straw lignin. The results also confirmed the increasing sugar content along with the occurrence of FA (Table 3 and Figure 2). Because the acylated ferulate can be incorporated into lignin by various coupling reactions such as  $\beta$ -5,  $\beta$ - $\beta'$ , and  $\beta$ -ether, the amount of FA was used to represent the maximum LCC value in wheat straw lignin. All evidence thus points out that the LCC in wheat straw is dominated by ferulate related linkages followed by minor amounts of benzyl ether and  $\gamma$ -ester linkages. Meanwhile, the preparation of MWL and CEL is necessary to completely reveal LCC structures in herbaceous biomass.<sup>8</sup>

**Analysis of Lignin Functional Groups.** Table 4 shows quantification of various functional groups (carbonyl, carboxylic, phenolic OH, aliphatic OH,  $\gamma$ -acylation, and methoxyl group) in isolated MWL and CEL analyzed by <sup>1</sup>H, <sup>13</sup>C, and HSQC NMR (Figure 5).

**Carbonyl Groups and Carboxylic Groups.** The range of  $\delta_C$  200–190 in <sup>13</sup>C NMR was assigned to conjugated aldehyde/keto including cinnamyl aldehyde and  $\alpha$ -keto in  $\beta$ -O-4 structures, which did not present obvious peaks in <sup>13</sup>C spectra (Figure 5). To eliminate the error caused by integration, the values of aldehyde from cinnamyl aldehyde and  $\alpha$ -keto in  $\beta$ -O-4 structures were estimated using the combination approach. The peak of 182 ppm was contributed by the carbonyl group on E

**Table 4. Quantification Analysis of Functional Groups (Carbonyl, Carboxylic, Phenolic OH, Aliphatic OH,  $\gamma$ -Acylation, and Methoxyl Group) by <sup>13</sup>C NMR Spectra, <sup>1</sup>H NMR Spectra, and Combination Analysis of <sup>13</sup>C and HSQC NMR Spectra of Wheat Straw Isolated MWL and CEL<sup>a</sup>**

| aliphatic region                                    | $\delta_C/\delta_H$                                     | MSL  | CEL  |
|---|---|------|------|
| <b>carbonyl groups</b>                              |   |      |      |
| cinnamyl aldehyde                                   | 153.5/7.62 <sup>c</sup>                                 | 0.1  | ND   |
| $\alpha$ -keto/ $\beta$ -O-4                        | 82.7/5.1 ( $\alpha$ -keto) <sup>c</sup>                 | 1.5  | 2.4  |
| C4 in E structure and quinone                       | 182.5–181.5 <sup>b</sup>                                | 4.5  | 5.2  |
| total   |   | 6.1  | 7.6  |
| <b>carboxylic groups</b>                            |   |      |      |
| aliphatic COOR                                      | 175–168 <sup>b</sup>                                    | 2.2  | 7.1  |
| conjugated COOR                                     | 168–166 <sup>b</sup>                                    | 4.2  | 7.8  |
| total   |   | 6.4  | 14.9 |
| <b>phenolic OH</b>                                  |   |      |      |
| unsaturated phenolic OH                             | 10.2–9.4 <sup>d</sup>                                   | 5.3  | 5.2  |
| saturated phenolic OH                               | 9.4–8.0 <sup>d</sup>                                    | 11.2 | 11.7 |
| free phenolic H units                               | 9.4–9.1 <sup>d</sup>                                    | 0.9  | 1.4  |
| free phenolic G units                               | 9.1–8.5 <sup>d</sup>                                    | 9.0  | 9.0  |
| free phenolic S and condensed free phenolic G units | 8.5–8.0 <sup>d</sup>                                    | 1.3  | 1.3  |
| total   |   | 16.5 | 16.9 |
| <b>aliphatic OH</b>                                 |   |      |      |
| $\alpha$ -OH in $\beta$ -O-4 structure              | 72.7–69.9/5.1–4.6 <sup>c</sup>                          | 28.3 | 33.8 |
| $\gamma$ -OH in $\beta$ -O-4 structure              | 62–60/4.2–4.0 <sup>c</sup>                              | 36.3 | 34.7 |
| $\gamma$ -OH in X1 structure                        | 62–58/3.8–3.0 <sup>c</sup>                              | 2.0  | 1.5  |
| total   |   | 66.6 | 70.0 |
| <b>acylation on <math>\gamma</math>-position</b>    | 60.8–58.8/3.8–3.35 <sup>c</sup>                         | 5.4  | 15.6 |
| <b>methoxyl groups</b>                              | 57.5–54 <sup>b</sup>                                    | 110  | 116  |
| <b>methoxyl groups</b>                              | theoretical methoxy calculated by S, G, T, and FA units | 110  | 112  |

<sup>a</sup>The amount of specific functional group was expressed as per 100 Ar.

<sup>b</sup>The specific region of <sup>13</sup>C NMR spectra. <sup>c</sup>The specific region of HSQC spectra. <sup>d</sup>The specific region of <sup>1</sup>H spectra.

and quinone. The minimal amount of carbonyl groups was approximately 6.1–7.6 units per 100 Ar in wheat straw lignin. The aliphatic COOR (integral at  $\delta_C$  175–168) and conjugated COOR groups ( $\delta_C$  168–166) were estimated by <sup>13</sup>C NMR. Wheat straw contained 14.9 and 6.4 carboxylic groups per 100 Ar in CEL and MSL, respectively (Table 4), which were significantly higher than woody samples (2–3 units of carboxylic groups per 100 Ar).<sup>4,5</sup> The increased amount of carboxylic groups in wheat straw lignin was ascribed to the existing FA content.

**Phenolic OH.** The chemical shift of phenolic OH was well assigned by investigating various model compounds in <sup>1</sup>H NMR.<sup>19</sup> The amount of unsaturated phenolic OH was estimated by integrating the range of 10.2–9.4 ppm, which was attributed to phenolic OH from FA, *p*CA, end group, and  $\alpha$ -oxidization lignin H/G/S. The aldehyde proton of cinnamyl aldehyde also partially overlapped in this area, which needed to be subtracted. The total amount of phenolic OH (approximately 5.0 units per 100 Ar) was close to corresponding amount of *p*CA in both MSL and CEL. The results implied that the unsaturated phenolic OH, at least the majority of them, may only arise from *p*CA. The saturated phenolic OH region



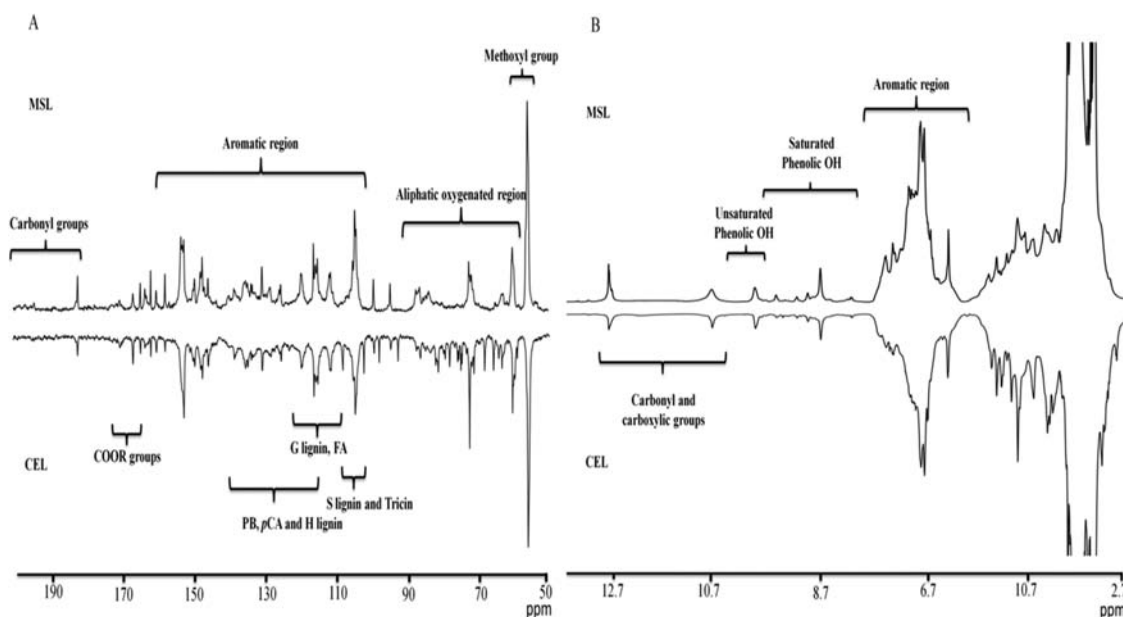


**Figure 5.** Quantitative  $^{13}\text{C}$  (A) and  $^1\text{H}$  (B) NMR spectra of MSL and CEL isolated from wheat straw.

(9.4–8.0 ppm) was assigned to phenolic H, G, and S units. The free phenolic S units partially overlapped with condensed free phenolic G units in the range of 8.5–8.0 ppm in the  $^1\text{H}$  NMR spectrum. Consistent with the dominance of G units in wheat straw lignin, the free phenolic G units were approximately 9 units per 100 Ar. The total phenolic OH were 16.5 and 16.9 units per 100 Ar for MSL and CEL, respectively.

**Aliphatic OH.** The total aliphatic OH was estimated by the sum of  $\alpha$ -OH in  $\beta$ -O-4 structures,  $\gamma$ -OH in  $\beta$ -O-4 structures, and  $\gamma$ -OH in X1 structures. Except for the  $\alpha$ -OH in  $\beta$ -O-4 structure, the amount of the other two groups has not been calculated in the analysis of the aliphatic region. The range of  $\delta_{\text{C}}/\delta_{\text{H}}$  62–58/3.8–3.0 and 62–60/4.2–4.0 was assigned to the  $\gamma$ -OH of X1 structures and the  $\gamma$ -OH of  $\beta$ -O-4 structures, respectively. Due to differences in  $T_2$  relaxation time, however, the amount of this structure was overestimated when compared to the internal reference:  $\delta_{\text{C}}/\delta_{\text{H}}$  113–109/7.6–6.8 cluster. To minimize this error, a new internal region,  $\delta_{\text{C}}/\delta_{\text{H}}$  66–58/4.5–3.0 cluster, was used. The results indicated that there were 2.0 and 1.5  $\gamma$ -OH per 100 Ar in X1 structures in MWL and CEL, which were comparable with a previous study.<sup>4</sup> The amount of X1 estimated by  $\gamma$ -OH content exceeded the estimation by its  $\beta$  correlations (Table 2). Therefore, the results suggested that  $\gamma$ -OH quantification of X1 structures may be a better representative for X1 content.

**Acylation on  $\gamma$ -OH.** One of the typical features in herbaceous lignin is the great acylation on lignin side chains.<sup>1</sup> A recent paper revealed the  $\gamma$ -OH of wheat straw lignin was partially acylated with acetates and pCAs on G units.<sup>15</sup> The results showed that CEL was highly acylated (15.6 units per 100 Ar) compared to MWL (5.4 units per 100 Ar). Similar values of pCA acylation were found in MWL, which suggested that acetate, which was previously detected in wheat straw lignin by DFRC degradation,<sup>15</sup> was present in low amounts, below the detection level of the NMR technique. On the contrary, the CEL contained approximately 8.9 acetates per 100 Ar obtained by total acylation units subtracted pCA and PB units.

**Methoxyl Groups.** The range of 57.5–54 ppm in  $^{13}\text{C}$  NMR was assigned to methoxyl groups. The results showed that wheat straw contained approximately 110–116 methoxyl groups per 100 Ar, which reflects changes in the S/G ratio. Because every S unit has two methoxyl groups, the cell wall with higher S/G ratio, such as hardwood (160 units per 100 Ar),<sup>5</sup> logically leads to higher methoxyl groups. However, G-rich plants, such as softwood (95 units per 100 Ar),<sup>4</sup> will contain fewer methoxyl groups. The theoretical amount of methoxyl groups in MSL and CEL was highly matched with the quantitation value, confirming the reliability of this method for evaluation of lignin units.

## ■ AUTHOR INFORMATION

### Corresponding Author

\*(S.C.) E-mail: chens@wsu.edu. Phone: 509-335-3743. Fax: 509-335-2722.

### Funding

We acknowledge the Agriculture Research Center, Washington State University, and the National Science Foundation (NSF Award 1231085) for providing financial support to this research.

### Notes

The authors declare no competing financial interest.

## ■ ACKNOWLEDGMENTS

We acknowledge Dr. John Ralph for discussion and suggestion.

## ■ REFERENCES

- (1) Buranov, A. U.; Mazza, G. Lignin in straw of herbaceous crops. *Ind. Crops Prod.* **2008**, *28*, 237–259.
- (2) Crestini, C.; Melone, F.; Sette, M.; Saladino, R. Milled wood lignin: a linear oligomer. *Biomacromolecules* **2011**, *12*, 3928–3935.
- (3) Bonawitz, N. D.; Chapple, C. The genetics of lignin biosynthesis: connecting genotype to phenotype. *Annu. Rev. Genet.* **2010**, *44*, 337–363.
- (4) Capanema, E. A.; Balakshin, M. Y.; Kadla, J. F. A comprehensive approach for quantitative lignin characterization by NMR spectroscopy. *J. Agric. Food Chem.* **2004**, *52*, 1850–1860.

- (5) Capanema, E. A.; Balakshin, M. Y.; Kadla, J. F. Quantitative characterization of a hardwood milled wood lignin by nuclear magnetic resonance spectroscopy. *J. Agric. Food Chem.* **2005**, *53*, 9639–9649.
- (6) del Río, J. C.; Prinsen, P.; Rencoret, J.; Nieto, L.; Jiménez-Barbero, J.; Ralph, J.; Martínez, A. T.; Gutiérrez, A. Structural characterization of the lignin in the cortex and pith of elephant grass (*Pennisetum purpureum*) stems. *J. Agric. Food Chem.* **2012**, *60*, 3619–3634.
- (7) Ralph, J.; Lu, F. The DFRC method for lignin analysis. 6. A simple modification for identifying natural acetates on lignins. *J. Agric. Food Chem.* **1998**, *46*, 4616–4619.
- (8) Balakshin, M.; Capanema, E.; Gracz, H.; Chang, H.; Jameel, H. Quantification of lignin–carbohydrate linkages with high-resolution NMR spectroscopy. *Planta* **2011**, *233*, 1097–1110.
- (9) Lapiere, C. Determining lignin structure by chemical degradations. In *Lignin and Lignans*; CRC Press: Boca Raton, FL, 2010; pp 11–48.
- (10) Ralph, J.; Landucci, L. NMR of lignins. In *Lignin and Lignans*; CRC Press: Boca Raton, FL, 2010; pp 137–243.
- (11) Schmidt, J. A. Electronic spectroscopy of lignins. In *Lignin and Lignans*; CRC Press: Boca Raton, FL, 2010; pp 49–102.
- (12) Peterson, D. J.; Loening, N. M. QQ-HSQC: a quick, quantitative heteronuclear correlation experiment for NMR spectroscopy. *Magn. Reson. Chem.* **2007**, *45*, 937–941.
- (13) Zhang, L.; Gellerstedt, G. Quantitative 2D HSQC NMR determination of polymer structures by selecting suitable internal standard references. *Magn. Reson. Chem.* **2007**, *45*, 37–45.
- (14) Crestini, C.; Argyropoulos, D. S. Structural analysis of wheat straw lignin by quantitative  $^{31}\text{P}$  and 2D NMR spectroscopy. The occurrence of ester bonds and  $\beta\text{-O-4}$  substructures. *J. Agric. Food Chem.* **1997**, *45*, 1212–1219.
- (15) del Río, J. C.; Rencoret, J.; Prinsen, P.; Martínez, A. T.; Ralph, J.; Gutiérrez, A. Structural characterization of wheat straw lignin as revealed by analytical pyrolysis, 2D-NMR, and reductive cleavage methods. *J. Agric. Food Chem.* **2012**, *60*, 5922–5935.
- (16) Sun, X.-F.; Sun, R.; Fowler, P.; Baird, M. S. Extraction and characterization of original lignin and hemicelluloses from wheat straw. *J. Agric. Food Chem.* **2005**, *53*, 860–870.
- (17) Sluiter, A.; Hames, B.; Ruiz, R.; Scarlata, C.; Sluiter, J.; Templeton, D.; Crocker, D. *Determination of Structural Carbohydrates and Lignin in Biomass*; Laboratory Analytical Procedure Technical Report NREL/TP-510-42618; NREL: Golden, CO, 2008 (revised July 2011).
- (18) Kim, H.; Ralph, J.; Akiyama, T. Solution-state 2D NMR of ball-milled plant cell wall gels in DMSO- $d_6$ . *BioEng Res.* **2008**, *1*, 56–66.
- (19) Li, S.; Lundquist, K. A new method for the analysis of phenolic groups in lignins by  $^1\text{H}$  NMR spectroscopy. *Nord. Pulp Pap. Res. J.* **1994**, *9*, 191–195.
- (20) Zhou, C.; Li, Q.; Chiang, V. L.; Lucia, L. A.; Griffis, D. P. Chemical and spatial differentiation of syringyl and guaiacyl lignins in poplar wood via time-of-flight secondary ion mass spectrometry. *Anal. Chem.* **2011**, *83*, 7020–7026.
- (21) Pan, X. J.; Sano, Y. Comparison of acetic acid lignin with milled wood and alkaline lignins from wheat straw. *Holzforschung* **2000**, *54*, 61–97.
- (22) Billa, E.; Koukios, E. G.; Monties, B. Investigation of lignins structure in cereal crops by chemical degradation methods. *Polym. Degrad. Stab.* **1998**, *59*, 71–75.
- (23) Day, A.; Ruel, K.; Neutelings, G.; Cronier, D.; David, H.; Hawkins, S.; Chabbert, B. Lignification in the flax stem: evidence for an unusual lignin in bast fibers. *Planta* **2005**, *222*, 234–245.
- (24) del Río, J. C.; Rencoret, J.; Gutiérrez, A.; Nieto, L.; Jiménez-Barbero, J.; Martínez, Á. T. Structural characterization of guaiacyl-rich lignins in flax (*Linum usitatissimum*) fibers and shives. *J. Agric. Food Chem.* **2011**, *59*, 11088–11099.
- (25) Li, L.; Zhou, Y.; Cheng, X.; Sun, J.; Marita, J. M.; Ralph, J.; Chiang, V. L. Combinatorial modification of multiple lignin traits in trees through multigene cotransformation. *Proc. Natl. Acad. Sci. U.S.A.* **2003**, *100*, 4939.
- (26) Scalbert, A.; Monties, B.; Lallemand, J. Y.; Guittet, E.; Rolando, C. Ether linkage between phenolic acids and lignin fractions from wheat straw. *Phytochemistry* **1985**, *24*, 1359–1362.
- (27) Ralph, J.; Landucci, L. NMR of lignins. In *Lignin and Lignans Advanced in Chemistry*; CRC Press: Boca Raton, FL, 2010; pp 137–243.
- (28) Lu, F.; Ralph, J. Detection and determination of *p*-coumaroylated units in lignins. *J. Agric. Food Chem.* **1999**, *47*, 1988–1992.
- (29) Hatfield, R.; Ralph, J.; Grabber, J. H. A potential role for sinapyl *p*-coumarate as a radical transfer mechanism in grass lignin formation. *Planta* **2008**, *228*, 919–928.
- (30) Bunzel, M.; Allerdings, E.; Ralph, J.; Steinhart, H. Cross-linking of arabinoxylans via 8-8-coupled diferulates as demonstrated by isolation and identification of di-arabinosyl 8-8 (cyclic)-dehydrodiferulate from maize bran. *J. Cereal Sci.* **2008**, *47*, 29–40.
- (31) Grabber, J. H.; Hatfield, R. D.; Ralph, J.; Zon, J.; Amrhein, N. Ferulate cross-linking in cell walls isolated from maize cell suspensions. *Phytochemistry* **1995**, *40*, 1077–1082.
- (32) Ralph, J.; Grabber, J. H.; Hatfield, R. D. Lignin-ferulate cross-links in grasses: active incorporation of ferulate polysaccharide esters into ryegrass lignins. *Carbohydr. Res.* **1995**, *275*, 167–178.
- (33) Sun, X. F.; Sun, R. C.; Fowler, P.; Baird, M. S. Extraction and characterization of original lignin and hemicelluloses from wheat straw. *J. Agric. Food Chem.* **2005**, *53*, 860–870.
- (34) Karhunen, P.; Rummakko, P.; Sipilä, J.; Brunow, G.; Kilpeläinen, I. Dibenzodioxocins; a novel type of linkage in softwood lignins. *Tetrahedron Lett.* **1995**, *36*, 169–170.
- (35) Zhang, L.; Gellerstedt, G.; Ralph, J.; Lu, F. NMR studies on the occurrence of spirodienone structures in lignins. *J. Wood Chem. Technol.* **2006**, *26*, 65–79.